Available online at www.sciencedirect.com
SCIENCE DIRECT®
Journal of Magnetism and Magnetic Materials 290–291 (2005) 750–753
journal of magnetism and magnetic materials
www.elsevier.com/locate/jmmm

Head-to-head domain walls in soft nano-strips: a refined phase diagram

Yoshinobu Nakatani[a,*], André Thiaville[b], Jacques Miltat[b]

[a]Department of Computer Science, University of Electro-Communications, 1-5-1 Chofugaoka, Chofu-shi, Tokyo 182-8585, Japan
[b]CNRS-Université Paris-sud, Laboratoire de physique des solides, Bât. 510, 91405 Orsay cedex, France

Available online 15 December 2004

Abstract

The wall structure phase diagram in nano-strips is established by numerical calculations, exhibiting a hitherto unknown wall type, the asymmetric transverse wall. The diagram of the wall-width parameter is obtained both from a one-dimensional fit of the wall structure and from the domain wall motion velocity under field, the latter being more relevant to experiments. These two estimates show some differences, which are understood using the definition of the effective wall width proposed by Thiele.

PACS: 75.60.Ch; 75.75.+a

Keywords: Domain wall structure; Domain wall energy; Domain wall width; Domain wall motion

Experimental results about domain wall (DW) motion in nanoscale magnetic strips under field or spin-polarized current injection were reported in recent years, fueled by the progress of nanoscale fabrication technology [1–4]. These results were compared with the equation for domain wall motion velocity, which was developed for the one-dimensional Bloch wall in perpendicular films (bubble materials) [5,6], namely $v = (\gamma\Delta/\alpha)H$, where γ is the gyromagnetic ratio, Δ the wall-width parameter (the Bloch wall width is $\pi\Delta$) and α the damping constant. It was shown earlier that this equation could be directly applied to the motion of transverse walls in narrow nano-strips [7], with a wall-width parameter Δ derived from numerical simulation. However, the nano-strips fabricated presently are often much wider than the exchange length, and a vortex wall may prove to be the stable structure. A phase diagram of domain wall structures in strips was previously reported [8] with, however, rather coarse steps in the parameter space and failing to investigate the wall-width parameter that is required for the estimation of the domain wall motion velocity. Furthermore, there exist some reports about transverse wall motion [9], but no precise report for the vortex wall.

In this paper, the phase diagram of the domain wall structure and the diagram of the wall-width parameter in Permalloy strips are obtained with a fine step by micromagnetic simulation. The motion of the vortex wall under field is also investigated.

Numerical methods are identical to those in Ref. [9]. The sample is divided into rectangular prisms with size $4 \times 4 \times h\,\mathrm{nm}^3$. The width w and thickness h of the strip are varied from 40 to 500 nm with 20 nm step and from 2 to 20 nm with 1 nm step, respectively. These correspond to the typical experimental values. The moving calculation region [9], always centered on the DW, is limited to a 2 μm length along the wire. The material parameters

*Corresponding author. Tel.:/fax: +81 424 43 5306.
E-mail address: nakatani@cs.uec.ac.jp (Y. Nakatani).

0304-8853/$ - see front matter © 2004 Elsevier B.V. All rights reserved.
doi:10.1016/j.jmmm.2004.11.355

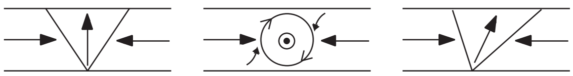

(a) TW (b) VW (c) ATW

Fig. 1. Domain wall structures in the magnetic nano-strips with longitudinal magnetization. (a) (symmetric) transverse wall, (b) vortex wall, (c) asymmetric transverse wall.

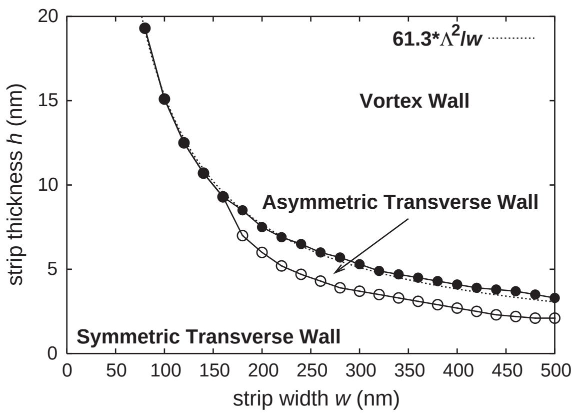

Fig. 2. Phase diagram of the domain wall structure in strips of Permalloy.

are: magnetization $M_s = 800\,\text{emu/cm}^3$, anisotropy $K_u = 0\,\text{erg/cm}^3$, exchange $A = 1 \times 10^{-6}\,\text{erg/cm}$, and damping $\alpha = 0.02$.

Fig. 1 schematizes the domain wall structures considered, the transverse wall (TW), the vortex wall (VW), and the asymmetric transverse wall (ATW). For all calculation conditions the VW and one TW could be obtained at equilibrium.

Fig. 2 displays the phase diagram of domain wall structures obtained by comparing the energy of the three domain walls. It shows that there is a region in which an ATW is stable, for a thickness in the interval 3–8 nm, in between the TW and VW stability areas. The TW–ATW transition appears to be of second order, the inclination angle of the wall behaving as $(h - h_c)^{1/6}$ for h above the transition thickness h_c (not shown). On the other hand, the transition (A)TW–VW is first order, giving rise to metastability as seen in Ref. [11]. The phase diagram previously reported, with coarser steps, only dealt with TW and VWs [8]. Our results show that the ATW area belongs to the TW area of the previous diagram. The figure also includes the equation of one phase boundary obtained in Ref. [8] which reproduces the results rather well.[1] We repeated the calculations with a three-dimensional model based on $4 \times 4 \times 4\,\text{nm}^3$ prisms in some cases, to check the accuracy of the calculation. The difference of the wall energies obtained by the two- and three-dimensional models was 4% at maximum.

[1]The coefficient of the equation was 128 in that paper, because of the different definition of the exchange length. We use the more standard form $\Lambda = (2A/\mu_0 M_s^2)^{1/2}$ [10].

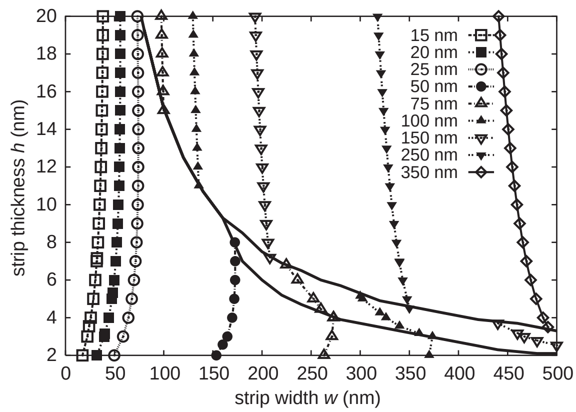

Fig. 3. Diagram of the wall-width parameter Δ fitted to the computed domain wall profiles (magnetization longitudinal component m_x). Some contours of constant Δ are drawn.

The wall-width parameter can, as done previously on very narrow strips [7], be first estimated by fitting the change of the x (wire direction) or y component (wire transverse direction) of the magnetic moment with the analytic form of the one-dimensional (1D) Bloch wall ($m_x = \tanh(x/\Delta)$, $m_y = 1/\cosh(x/\Delta)$). As the magnetization may vary sizeably along the transverse direction in the computed domain wall structures, averaged values along this direction are used for fitting. Fig. 3 shows the resulting diagram. The Δ parameter increases with strip width, but depends weakly on the strip thickness both for TW and VWs. TW and VW widths are very different, as one has nearly $\pi\Delta = w$ for the TW and $\Delta = 3w/4$ for the VW. In the ATW case, Δ increases with increasing strip width and thickness.

Next, an external field is applied along the strip length in order to obtain the velocity of the domain wall motion. Fig. 4 shows the effect of various parameters on the velocity vs. field relation in a 240 nm wide strip. Velocity increases with field up to the Walker field, and drops suddenly afterwards because of the periodic nucleation and annihilation of antivortices [9]. The deviation from linearity, below the Walker field, arises from the wall-width reduction due to out of plane precession of the domain wall moments. Note that the velocity increases further again for very thin films ($h = 2\,\text{nm}$). In that case the just-created antivortex gets quickly separated from the main domain wall so that the velocity is hardly affected.

The velocity and the Walker field decrease with increasing strip thickness. This can be explained as follows. The magnetic moments in the wall acquire a component perpendicular to the strip plane by

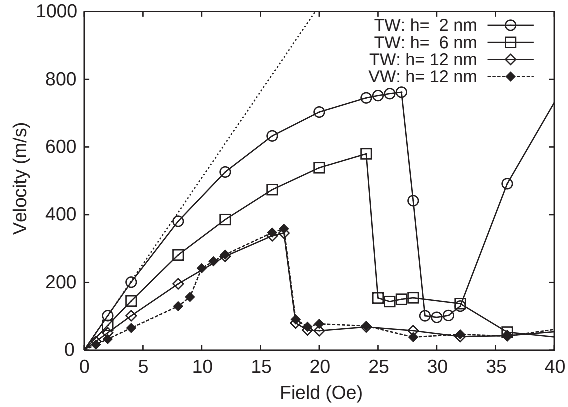

Fig. 4. Effect of field, strip thickness and wall structure on the wall motion velocity. The width of the strip is 240 nm. The tangent (dotted) line to the $h = 2$ nm curve corresponds to $\Delta = 57.8$ nm, close to the value $\Delta = 69.7$ nm determined in Fig. 3.

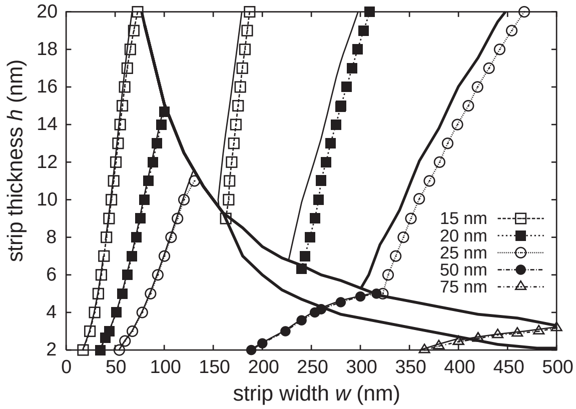

Fig. 5. Diagram of the "dynamic" wall-width parameter obtained from the domain wall motion velocity, shown by various lines of constant value (symbols). The corresponding continuous lines were obtained with Thiele's definition (1) of the wall width.

precession around the external field. This component gives rise to a demagnetizing field in the perpendicular direction, the wall now moving via the precession of magnetic moments around that field. Therefore, the demagnetizing field in the perpendicular direction is the direct driving field for the domain wall motion. This field also tends to oppose vortex nucleation. The value of the demagnetizing field is at most $4\pi M_s$, and decreases as the thickness is increased (finite aspect ratio effect), which explains the observed tendencies.

The velocity of the VW is lower than that of the TW, because of increased energy dissipation at the vortex core [6]. Velocities become identical at fields larger than 9 Oe, as the vortex is expelled by the so-called gyrotropic force [6] and an ATW appears. Also note that the applied field pushes directly the vortex core out of the strip. One sees additionally in Fig. 4 that the mobility decreases steadily with increasing strip thickness, a behaviour at variance to that expected from Fig. 3: only at the lowest thickness $h = 2$ nm are the values (in terms of the wall width parameter Δ) close. These results show that the wall-width parameter, when obtained by fitting the one-dimensional model to the domain wall structure, can be used to estimate the domain wall velocity for small fields only for very narrow strips. In general, the effective wall-width parameter obtained from the domain wall motion velocity, $\Delta_{\mathrm{eff}} = v\alpha/\gamma H$, is required.

Fig. 5 shows the "dynamic" diagram of the effective wall-width parameter. The simulations of the domain wall motion were performed with a 1 Oe external field so as to avoid the change of the domain wall structure. The duration of the simulation was varied from 10 to 200 ns, because very long simulation times were required to obtain the steady-state motion under small external fields. In the diagram, Δ_{eff} increases as the strip width is increased. However, it decreases with increasing thickness, because the internal driving field decreases. The parameter of the VW is smaller than that of the TW with the same strip width because of the core effect mentioned above. Moreover, whereas Fig. 3 showed a break in the slope of the level lines at the TW to ATW transition, there is no discontinuity here because a moving TW tilts under increased dissipation on its thinner side.

Comparison of Figs. 3 and 5 shows that they agree only for thin strips ($w < 30$ nm), where the one-dimensional model is valid. Outside this region, one has to use the definition proposed by Thiele [12] in its analysis of stationary motion of general magnetic structures

$$2/\Delta = (1/w) \int (\partial \mathbf{m}/\partial x)^2 \, \mathrm{d}x \, \mathrm{d}y. \quad (1)$$

The continuous lines in Fig. 5, obtained from Eq. (1), realize now a much better agreement.

In conclusion, the data presented in Figs. 4 and 5 allow for a proper interpretation of wall mobility experiments in nanostrips.

References

[1] T. Ono, et al., Science 248 (1999) 468.
[2] D. Atkinson, et al., Nat. Mater. 2 (2003) 85.
[3] N. Vernier, et al., Europhys. Lett. 65 (2004) 526.
[4] A. Yamaguchi, et al., Phys. Rev. Lett. 92 (2004) 077204.
[5] N.L. Schryer, L.R. Walker, J. Appl. Phys. 45 (1974) 5406.
[6] A.P. Malozemoff, J.C. Slonczewski, Magnetic Domain Walls in Bubble Materials, Academic Press, New York, 1979.

[7] A. Thiaville, et al., J. Magn. Magn. Mater. 242–245 (2002) 1061.
[8] R.D. McMichael, M.J. Donahue, IEEE Trans. Magn. 33 (1997) 4167.
[9] Y. Nakatani, et al., Nat. Mater. 2 (2003) 521.
[10] A. Hubert, R. Schäfer, Magnetic Domains, Springer, Berlin, 1998.
[11] M. Kläui, et al., J. Magn. Magn. Mater.
[12] A.A. Thiele, Phys. Rev. Lett. 30 (1973) 230.